Circuit modeling of the transmissivity of stacked two-dimensional metallic meshes

Chandra S. R. Kaipa,[1] Alexander B. Yakovlev,[1] Francisco Medina[2,*], Francisco Mesa,[2] Celia A. M. Butler,[3] and Alastair P. Hibbins[3]

[1]*Dept. of Electrical Engineering, University of Mississippi, University, MS 38677-1848, USA*
[2]*Microwave Group, University of Seville, Seville, 41012, Spain*
[3]*Electromagnetic Materials Group, School of Physics, University of Exeter, Exeter, Devon, EX4 4QL, UK*
**medina@us.es*

Abstract: This paper presents a simple analytical circuit-like model to study the transmission of electromagnetic waves through stacked two-dimensional (2-D) conducting meshes. When possible the application of this methodology is very convenient since it provides a straightforward rationale to understand the physical mechanisms behind measured and computed transmission spectra of complex geometries. Also, the disposal of closed-form expressions for the circuit parameters makes the computation effort required by this approach almost negligible. The model is tested by proper comparison with previously obtained numerical and experimental results. The experimental results are explained in terms of the behavior of a finite number of strongly coupled Fabry-Pérot resonators. The number of transmission peaks within a transmission band is equal to the number of resonators. The approximate resonance frequencies of the first and last transmission peaks are obtained from the analysis of an infinite structure of periodically stacked resonators, along with the analytical expressions for the lower and upper limits of the pass-band based on the circuit model.

OCIS codes: (050.1950) Diffraction and gratings; (050.6624) Subwavelength structures; (050.2230) Fabry-Pérot.

References and links

1. E. Yablonovitch, "Inhibited spontaneous emission in solid-state physics and electronics," Phys. Rev. Lett. **58**, 2059–2062 (1987).
2. S. John, "Strong localization of photons in certain disordered dielectric superlattices," Phys. Rev. Lett. **58**, 2486–2489 (1987).
3. M. Scalora, M. J. Bloemer, A. S. Pethel, J. P. Dowling, C. M. Bowden, and A. S. Manka, "Transparent, metallo-dielectric, one-dimensional, photonic band-gap structures," J. Appl. Phys. **83**, 2377–2383 (1998).
4. M. R. Gadsdon, J. Parsons, and J. R. Sambles, "Electromagnetic resonances of a multilayer metal-dielectric stack," J. Opt. Soc. Am. B **26**, 734–742 (2009).
5. S. Feng, J. M. Elson, and P. L. Overfelt, "Transparent photonic band in metallodielectric nanostructures," Phys. Rev. B **72**, 085117 (2005).
6. M. C. Larciprete, C. Sibilia, S. Paoloni, and M. Bertolotti, "Accessing the optical limiting properties of metallo-dielectric photonic band gap structures," J. Appl. Phys. **93**, 5113–5017 (2003).
7. I. R. Hooper and J. R. Sambles, "Some considerations on the transmissivity of thin metal films," Opt. Express **16**, 17249–17256 (2008).
8. C. A. M. Butler, J. Parsons, J. R. Sambles, A. P. Hibbins, and P. A. Hobson, "Microwave transmissivity of a metamaterial-dielectric stack," Appl. Phys. Lett. **95**, 174101 (2009).

#125055 - $15.00 USD Received 4 Mar 2010; revised 26 May 2010; accepted 4 Jun 2010; published 7 Jun 2010

9. A. B. Yakovlev, C. S. R. Kaipa, Y. R. Padooru, F. Medina, and F. Mesa, "Dynamic and circuit theory models for the analysis of sub-wavelength transmission through patterned screens," in *3rd International Congress on Advanced Electromagnetic Materials in Microwaves and Optics*, (London, UK, 2009), pp. 671–673.
10. T. W. Ebbesen, H. J. Lezec, H. F. Ghaemi, T. Thio, and P. A. Wolff, "Extraordinary optical transmission through sub-wavelength hole arrays," Nature (London) **391**, 667–669 (1998).
11. R. E. Collin, *Field Theory of Guided Waves* (IEEE Press, 1991).
12. B. A. Munk, *Frequency Selective Surfaces: Theory and Design* (Wiley, 2000).
13. R. Ulrich, "Far-infrared properties of metallic mesh and its complementary structure," Infrared Phys. **7**, 37–55 (1967).
14. R. Sauleau, Ph. Coquet, J. P. Daniel, T. Matsui, and N. Hirose, "Study of Fabry-Pérot cavities with metal mesh mirrors using equivalent circuit models. Comparison with experimental results in the 60 GHz band," Int. J. Infrared and Millim. Waves **19**, 1693–1710 (1998)
15. O. Luukkonen, C. Simovski, G. Granet, G. Goussetis, D. Lioubtchenko, A. V. Raisanen, and S. A. Tretyakov, "Simple and analytical model of planar grids and high-impedance surfaces comprising metal strips or patches," IEEE Trans. Antennas Propag. **56**, 1624–1632 (2008).
16. F. Medina, F. Mesa, and R. Marqués, "Extraordinary transmission through arrays of electrically small holes from a circuit theory perspective," IEEE Trans. Microwave Theory Tech. **56**, 3108–3120 (2008).
17. F. Medina, F. Mesa, and D. C. Skigin, "Extraordinary transmission through arrays of slits: a circuit theory model," IEEE Trans. Microwave Theory Tech. **58**, 105–115 (2010).
18. N. Engheta, A. Salandrino, and A. Alu, "Circuit elements at optical frequencies: nanoinductors, nanocapacitors, and nanoresistorsExtraordinary transmission through arrays of," Phys. Rev. Lett. **95**, 095504 (2005).
19. A. Alu, M. E. Young, and N. Engheta, "Design of nanofilters for optical nanocircuits," Phys. Rev. B **77**, 144107 (2008).
20. S. Tretyakov, *Analytical modeling in applied electromagnetics*, (Artech House, 2003).
21. HFSS: High Frequency Structure Simulator based on the Finite Element Method, Ansoft Corporation, http://www.ansoft.com
22. D. M. Pozar, *Microwave Engineering*, third edition, (Wiley, 2004).
23. CST Microwave Studio CST GmbH, Darmstadt, Germany, 2008, http://www.cst.com.

1. Introduction

The use of periodic structures to control electromagnetic wave propagation and energy distribution is nowadays a common practice in optics and microwaves research. Since the introduction of photonic band-gap structures (PBG's) by the end of 1980's [1, 2], hundreds of papers have been published exploring the theoretical challenges and practical realizations of such kind of structures. Although most of the published papers dealt with 3-D periodic distributions of refraction index, 1-D periodic structures have also attracted a lot of interest in the optics community. The analysis of 1-D structures requires much less computational resources, while such structures still exhibit many of the salient features observed in 3-D photonic crystals. Moreover, 1-D periodic structures are interesting *per se* due to their practical applications in layered optical systems. For instance, although extremely thin metal layers are highly reflective at optical frequencies, the superposition of a number of these layers separated by optically thick transparent dielectric slabs has been shown to generate high transmissivity bands [3, 4]. Although Fabry-Pérot (FP) resonances can be invoked as the underlying mechanism behind this enhanced transmissivitty, it will be explained in this paper that PBG theory can also be used if the number of unit cells is large (each unit cell involves a thin metal film together with a thick dielectric slab). When the number of unit cells is finite, the transmission spectrum for each transmission band presents a number of peaks equal to the number of FP resonators that can be identified in the system. (Totally transparent bands without peaks have also been reported [5], although that interesting case will not be considered in this paper). The highest frequency peak is associated with a low field density inside the metal films, while the lowest frequency peak corresponds to a situation where field inside the metal layers is relatively strong (the possibility of achieving field enhancement inside a nonlinear region using those stacked structures has been explored in [6]). However, all these interesting properties are lost at lower frequencies, below a few dizaines of THz. This is because electromagnetic waves inside metals at optical frequencies exist in the

#125055 - $15.00 USD Received 4 Mar 2010; revised 26 May 2010; accepted 4 Jun 2010; published 7 Jun 2010

form of evanescent waves (the real part of the permittivity of a metal at optical frequencies is relatively large and negative, the imaginary part being smaller or of the same order of magnitude). These evanescent waves provide the necessary coupling mechanism between successive dielectric layers (Fabry-Pérot resonators) separated by metal films. At lower frequencies, metals are characterized by their high conductivities (or equivalently, large imaginary dielectric constants), in such a way that almost perfect shielding is expected even for extremely thin films a few nanometers thick [7]. Therefore, the method reported in [3,4,6] cannot be used in practice to enhance transmission at microwave or millimeter-wave frequencies.

However, the authors have recently proposed physical systems that mimic the observed behavior of stacked metal-dielectric layers at optical frequencies, but in the microwave region of the spectrum [8, 9]. In these systems, the metal films found in optical experiments are substituted by perforated metal layers (2-D metallic meshes). The resulting metal-dielectric stacked structure is shown in Fig. 1. In this work, the period of the distribution of square holes and the holes themselves are small in comparison with the free-space wavelength of the radiation used in the experiments and simulations. Since we operate in the non-diffracting regime, surface waves cannot be diffractively excited to induce enhanced transmission phenomena such as those reported in [10]. Due to the small electrical size of the lattice constant of the mesh, very poor transmission is expected for every single grid, alike the metallic films of the above mentioned optical systems. However, the grid provides a mechanism for excitation of evanescent fields. If the operation frequency is low enough, as it is the case considered in this letter, the evanescent fields are predominantly inductive (*i.e.*, the magnetic energy stored in the reactive fields around the grid is higher than the electric energy). Therefore, the effective electromagnetic response of the mesh layer is similar to that of Drude metals in the visible regime. If a number of periodically perforated metallic screens is stacked as shown in Fig. 1, the situation resembles the original optical problem previously discussed. The difference is that, in the microwave range, the reactive fields spread around the holes of the perforated screens while they are confined into the metallic films in the optical range. However, if the separation between successive metallic meshes is large enough (roughly speaking, larger than the periodicity of the mesh itself), evanescent fields generated at each grid do not reach the adjacent ones. In such situation a full analogy can be found between the stacked slabs in the optical system and the stacked meshes in the microwave system. Such analogy was confirmed through the experiments and finite-element simulations in [8]. However, periodic structures (with periodicity along the propagation direction or along the direction perpendicular to propagation) have been analyzed in the microwave and antennas literature for several decades using circuit models [11, 12]. Indeed, problems closely related to the one treated in this work have been analyzed following the circuit approach in [13, 14], for instance. More recently, 2-D periodic high-impedance surfaces have also been analyzed following the circuit-theory approach [15]). Even the extraordinary transmission phenomena observed through perforated metal films (which are associated with the resonant excitation of bound surface waves [10]) have been explained in terms of circuit analogs with surprisingly accurate results [16, 17]. Since circuit models provide a very simple picture of the physical situation and demand negligible computational resources, we will explore these advantanges to explain the behavior of stacked grids. However, it should be mentioned that the use of that circuit modeling can also be used at optical frequencies. For instance, the functionality of inductors, capacitors or resistors can be implemented at optical frequencies using plasmonic and non plasmonic nanoparticles [18]. Complex electrical responses, such as those of filters of different types, can be achieved using the behavior of metals at optical frequencies and suitable geometries [19]. As it will be explained later, the concepts introduced in [18, 19] together with the theory in this paper can explain the results reported in [4]. This is due to the similar physical responses of the inductive loading provided by the subwavelength

#125055 - $15.00 USD Received 4 Mar 2010; revised 26 May 2010; accepted 4 Jun 2010; published 7 Jun 2010

grids in [8] and the negative permittivity of the metal films in [4].

In this paper, our first goal here is to show how a circuit model, whose parameters are analytically known, reasonably accounts for the experimental and numerical results reported in [8]. As stated above, this methodology is a common practice in microwave engineering and the reader can find a systematic and elegant description in a relatively recent book by S. Tretyakov [20]. Apart from avoiding lengthy and cumbersome computations, the circuit modeling provides additional physical insight and, most importantly, a methodology to design devices based on the physical phenomena described by the model. The circuit approach is also used to extract some general features of the transmission frequency bands through the analysis of an infinite structure with periodically stacked unit cells along the direction of propagation. The relation between the finite and the infinite structures is studied in the light of the equivalent circuit modeling technique.

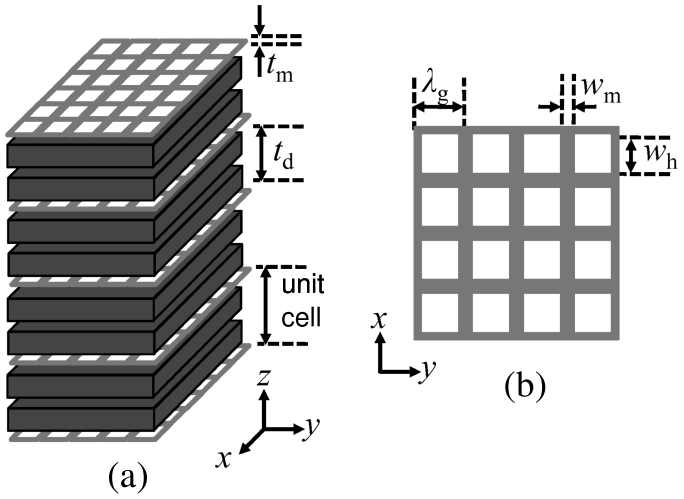

Fig. 1. (a) Exploded schematic (the air gaps between layers are not real) of the five stacked copper grids separated by dielectric slabs used in the experiments reported in [8]. This is an example of the type of structure for which the model in this paper is suitable. (b) Top view of each metal mesh.

2. Stacked grids and unit cell model

An example of the kind of structures analyzed in this paper is given in Fig. 1. The system is composed by a set of stacked metallic grids printed on dielectric slabs. This is the multilayered structure fabricated and measured by some of the authors of this paper in [8]. Five copper grids, printed on a low-loss dielectric substrate using a conventional photo-etching process, are stacked to produce an electrically thick block, whose transmission characteristics at microwave frequencies are the subject of this study. The copper cladding thickness is $t_m = 18\,\mu$m, and the thickness of each of the low-loss dielectric slabs (Nelco NX9255) separating copper meshes is $t_d = 6.35$ mm. The relative permittivity of the dielectric material is $\varepsilon_r \approx 3$. The loss tangent used in our simulations is $\tan\delta = 0.0018$. The lattice constant of the grid is $\lambda_g = 5.0$ mm, and the side length of square holes is $w_h = 4.85$ mm (thus the metallic strips conforming the mesh are $w_m = 0.15$ mm wide). When a y-polarized (or x-polarized wave) uniform transverse electromagnetic plane wave normally impinges on the structure, the fields are identical for each of the unit cells of the 2-D periodic system. Taking into consideration the symmetry of the unit

#125055 - $15.00 USD Received 4 Mar 2010; revised 26 May 2010; accepted 4 Jun 2010; published 7 Jun 2010

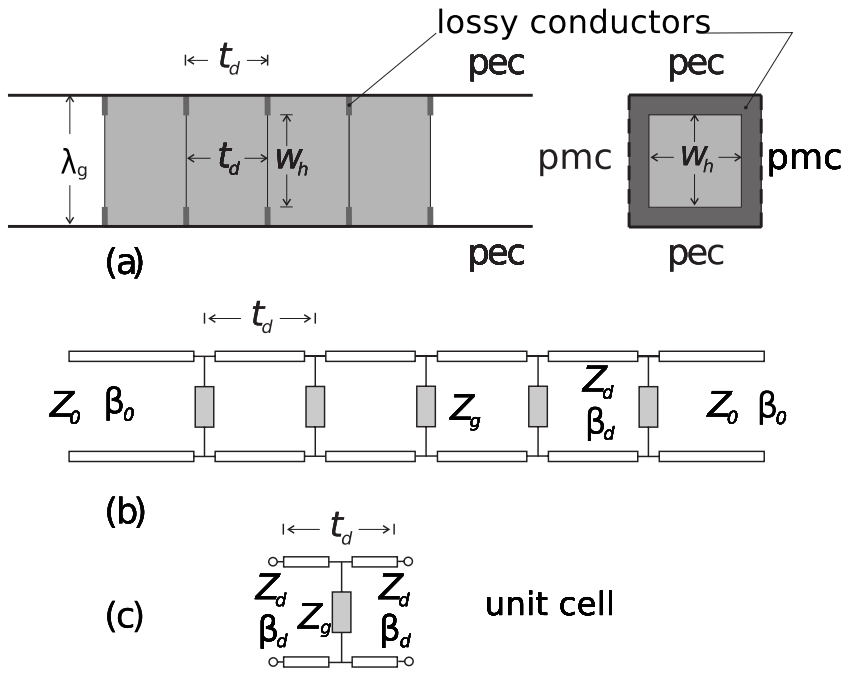

Fig. 2. (a) Transverse unit cell of the 2-D periodic structure corresponding to the analysis of the normal incidence of a *y*-polarized uniform plane wave on the structure shown in Fig. 1 (pec stands for perfect electric conductor, and pmc stands for perfect magnetic conductor). (b) Equivalent circuit for the electrically small unit cell (λ_g meaningfully smaller than the wavelength in the dielectric medium surrounding the grids); Z_0 and β_0 are the characteristic impedance and propagation constant of the air-filled region (input and output waveguides); Z_d and β_d are the same parameters for the dielectric-filled region (real for lossless dielectric and complex for lossy material). (c) Unit cell for the circuit based analysis of an infinite periodic structure.

cell and the polarization of the impinging electric field, a single unit cell such as that shown in Fig. 2 can be used in the analysis. Thus, we have a number of uniform sections equivalent to parallel-plate waveguides, filled with air or with the above mentioned dielectric material, separated by diaphragm discontinuities. This is a typical waveguide problem with discontinuities, as those commonly considered in microwave engineering practice [11]. Since a single transverse electromagnetic (TEM) mode is assumed to propagate along the uniform waveguide sections (higher-order modes operate below their cutoff frequencies, or equivalently, it is assumed a non-diffacting regime), the circuit model shown in Fig. 2(b) gives an appropriate description of the physical system in Fig. 2(a). The shunt reactances in this circuit account for the effect of the below-cutoff higher-order modes scattered by each of the discontinuities. This model is valid provided the attenuation factor of the first higher-order mode generated at the discontinuities is large enough to ensure the interaction between successive discontinuities through higher-order modes can be neglected. The first higher-order modes that can be excited by the highly symmetrical holes under study are the TM_{02} and TE_{20} parallel-plate waveguide modes (TM/TE stands for transverse magnetic/electric to the propagation direction). The cutoff wavelength for these modes is $\lambda_c = \lambda_g$. The attenuation factor for frequencies not too close to cutoff ($f_c \approx 60\,\text{GHz}$ for the air-filled waveguides and $34.7\,\text{GHz}$ for the dielectric-filled sections) is $\alpha_{\text{TM}_{02}} = \alpha_{\text{TE}_{20}} \approx 2\pi/(\sqrt{\varepsilon_r}\lambda_g)$. Since $\lambda_g = 5.0\,\text{mm}$ and the separation between the perforated

#125055 - $15.00 USD Received 4 Mar 2010; revised 26 May 2010; accepted 4 Jun 2010; published 7 Jun 2010

screens is 6.35 mm, the amplitude of the higher-order modes excited by each discontinuity at the plane of adjacent discontinuities is clearly negligible. Thus, the simple circuit in Fig. 2(b) should be physically suitable for our purposes as long as the interaction between adjacent diaphragms takes place, exclusively, through the transverse electromagnetic waves represented by the transmission line sections.

The parameters of the transmission lines in Fig. 2(b), propagation constants (β_0 for air-filled sections and β_d for dielectric-filled sections) and characteristic impedances (Z_0 and Z_d), are known in closed form. The expressions for those parameters are

$$\beta_0 = \frac{\omega}{c} \;\; ; \;\; \beta_d = \sqrt{\varepsilon_r(1 - j\tan\delta)}\,\beta_0 \tag{1}$$

$$Z_0 = \sqrt{\frac{\mu_0}{\varepsilon_0}} \;\; ; \;\; Z_d = \sqrt{\frac{\mu_0}{\varepsilon_0}}\frac{1}{\sqrt{\varepsilon_r(1 - j\tan\delta)}} \tag{2}$$

where ω is the angular frequency and c the speed of light in vacuum. Note that, due to losses, Z_d and β_d are complex quantities with small (low-loss regime) but non-vanishing imaginary parts.

Unfortunately, no exact closed-form expressions are available for the reactive loads, Z_g, in Fig. 2(b). As mentioned before, these lumped elements account for the effect of below-cutoff higher-order modes excited at the mesh plane. A relatively sophisticated numerical code could be used to determine these parameters. In such case, however, no special advantage would be obtained from our circuit analog, apart from a different point of view and some additional physical insight. However, for those frequencies making the size of the unit cell, λ_g, electrically small, accurate estimations for Z_g are available in the literature. For $w_m \ll \lambda_g$ the grid mainly behaves as an inductive load with the following impedance for normal incidence [15]:

$$Z_g = j\omega L_g \;\; ; \;\; L_g = \frac{\eta_0\lambda_g}{2\pi c}\ln\left[\csc\left(\frac{\pi w_m}{2\lambda_g}\right)\right] \tag{3}$$

where $\eta_0 = \sqrt{\mu_0/\varepsilon_0} \approx 377\,\Omega$ is the free-space impedance. Ohmic losses can also be taken into account using the surface resistance of the metal (copper), since the skin effect penetration depth, $\delta_s = \sqrt{2/(\omega\mu_0\sigma)}$, is much smaller than the thickness of the metal strips in our case. This resistance, series connected with the inductance in (3), is given by $R_g = \lambda_g/(\sigma w_m \delta_s)$.

Since the formulas for Z_g are not exact and the model has some limitations (for instance, the unit cell has to be electrically small enough), the predictions of our model must be checked against experimental and/or numerical results. This will be done in the forthcoming section.

3. Comparison with numerical and experimental data

As a first test for our model, in Fig. 3 we compare its predictions with the numerical and experimental results reported in [8] for the transmissivity of the five stacked grids studied in that paper. Experimental, numerical (simulations based on the finite elements method implemented into the commercial code [21]), and analytical (circuit-model predictions) results are included in this figure. We can clearly appreciate how two bands, consisting of two groups of four transmission peaks separated by a deep stop band, are predicted by the present analytical model, in agreement with the experimental results in [8] (no HFSS simulations were reported for the second band in that paper). In the frequency range where the metal mesh is reasonably expected to behave as a purely inductive grid (well below the onset of the first higher-order mode in the dielectric-filled sections, at approximately 34.7 GHz for the dielectric material and cell dimensions involved in this example), the quantitative agreement between analytical and experimental/numerical data is very good. The quality of the analytical results, however, deteriorates

#125055 - $15.00 USD Received 4 Mar 2010; revised 26 May 2010; accepted 4 Jun 2010; published 7 Jun 2010

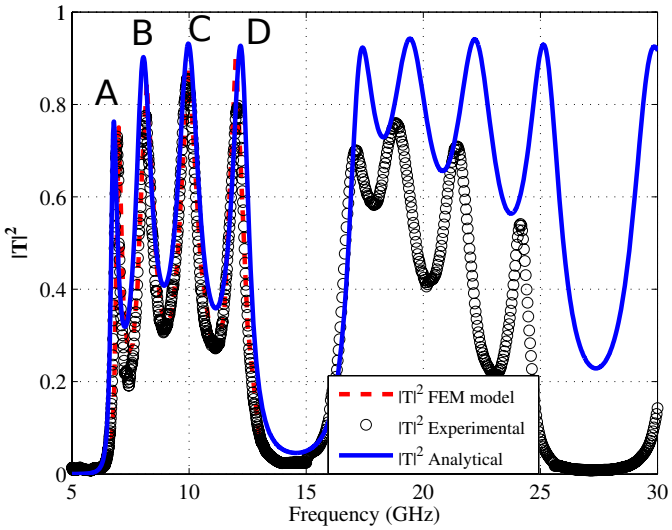

Fig. 3. Transmissivity ($|T|^2$) of the stacked grids structure experimentally and numerically studied in [8]. HFSS (FEM model, FEM standing for finite elements method) and circuit simulations (analytical data) are obtained for the following parameters [with the notation used in Fig. 1]: $\lambda_g = 5.0\,\text{mm}$, $w_m = 0.15\,\text{mm}$, $t_d = 6.35\,\text{mm}$, $t_m = 18\,\mu\text{m}$; metal is copper and the dielectric is characterized by $\varepsilon_r = 3$ and $\tan\delta = 0.0018$. The four resonant modes in the first band are labeled as A, B, C, and D in the increasing order of frequency.

when the frequency increases (second band). A possible explanation for the disagreement is that the inductive model is not expected to capture the behavior of the near field around the strip wires at the higher frequencies of the second transmission band (it can be conjectured that capacitive effects cannot be ignored at high frequencies). Indeed, the effect of adding a small shunt capacitance would be to slightly shift the peaks to lower frequencies, thus improving the qualitative matching to experimental results. Unfortunately, no closed form expression has been found for that capacitance. On the other hand, dielectric losses at that frequency region appears to be higher than expected from the loss tangent used in the circuit simulation (nominal value for the commercial substrate). Likely, loss tangent of the dielectric slab is much higher than supposed, in such a way that the height of transmission peaks could be adequately predicted wiht our model provided the true loss tangent is used in the simulation. In spite of these quantitative discrepancies affecting the high frequency portion of the transmission spectrum, reasonable qualitative agreement can still be observed even in the second transmission band (four transmission peaks distributed along, approximately, the same frequency range for the analytical model and measured data). This is because the model in Fig. 2 is still valid at those frequencies, except for the effects above mentioned (Z_g should be different and losses higher). Nevertheless, the essential fact is not modified: we have four FP cavities strongly coupled through the square holes of each grid; *i.e.*, four transmission line sections separated by predominantly reactive impedances. Note that this point of view is somewhat different and alternative to that sustained in [8], which is based on the interaction between the standing waves along the dielectric regions and the evanescent waves in the grid region, although compatible with it. The difference is that the evanescent fields are not considered to be exclusively confined to the interior of the holes (which are regarded in [8] as very short sections of square waveguides operating below cutoff or, equivalently, as imaginary-index regions). The reactive fields yielding the reactive load, Z_g,

#125055 - $15.00 USD Received 4 Mar 2010; revised 26 May 2010; accepted 4 Jun 2010; published 7 Jun 2010

are now considered to extend over a certain distance, from the position of each grid, inside the dielectrics. Under the present point of view, the thicknesses of the grids are not relevant if they are sufficiently small, and they can be considered zero for practical purposes. It is worth mentioning that the circuit model developed for the present microwave structure could also be applied to study the stacked slabs reported in [4]. The reason is that the narrow metal films having negative permittivity are expected to behave as lumped inductors following the theory in [18, 19]. Note that the model in this paper should be modified (and the transmission spectrum would be different too) if the distance between grids were much smaller than considered. In such case the interaction due to higher order modes should be incorporated in the model, but this is not a trivial task and it is beyond the scope of the present paper. However, this problem would not affect to the optical structure analyzed in [4] because in that structure only TEM waves are excited at the interfaces between metal films and dielectric slabs, and they can be taken into account in closed form. This is an important simplifying difference with respect to the problem treated in this paper.

4. Field distributions for the resonance frequencies

It is important to verify if the field distribution predicted by the circuit model agrees with that provided by numerical simulations based on HFSS. Being a 3-D finite element method solver, HFSS gives information about the fields at any point within the unit cell of the structure. Certainly this is beyond the possibilities of a one-dimensional circuit model. However, the circuit model can give information about the line integral of the field along any line going from the top to the bottom metal plates of each of the parallel-plate waveguides for each particular value of z (*i.e.*, voltage or, conversely, average value of the electric field). Thus, the comparison between circuit model and HFSS results can easily be carried out because our average values of electric field can be compared, after proper normalization, with the values reported in [8] for the field along a line plotted in the z-direction through the center of a hole. It is worthwhile to consider how each of the four resonance modes in the first high transmissivity frequency band (labeled as A, B, C, and D in Fig. 3) is associated with a specific field pattern along the propagation direction (z). The results for these field distributions are plotted in Fig. 4. The first obvious conclusion is that the circuit model, once again, captures the most salient details of the physics of the problem, with the advantage of requiring negligible computational resources. Slight differences can be appreciated around the grid positions because, in a close proximity to the grids, HFSS provides results for the near field (which plays the role of the *microscopic* field in the continuous medium approach) while the analytical model gives a *macroscopic* field described by the transverse electromagnetic waves. Microscopic and macroscopic fields averaged over the lattice period are comparable for sub-wavelength grids considered in this paper. Nevertheless, with independence of the model (numerical or analytical), we can see how the field values near and over each of the three internal grids are meaningfully different for each of the considered resonance (high transmission) frequencies. The field values are relatively small over each of those internal grids for mode D. For mode C we have two grids with low field levels, and for mode B only the central grid has low values of electric field. Finally, none of the internal grids have low electric field values for mode A. The effect of an imaginary impedance at the end of a transmission line section with a significant voltage excitation is to increase the apparent (or equivalent) length of that section, as it has been explained in detail in [17] for a different system having a similar equivalent circuit (resonant slits in a metal screen). The above reason explains why the resonance frequencies of the modes with more highly excited discontinuities have smaller resonance frequency. In general, this discussion is compatible with that given in [8] about the distribution of peaks. However, some further details can be clarified using the circuit model; for instance, those concerning the positions of the first and last resonance and

#125055 - $15.00 USD Received 4 Mar 2010; revised 26 May 2010; accepted 4 Jun 2010; published 7 Jun 2010

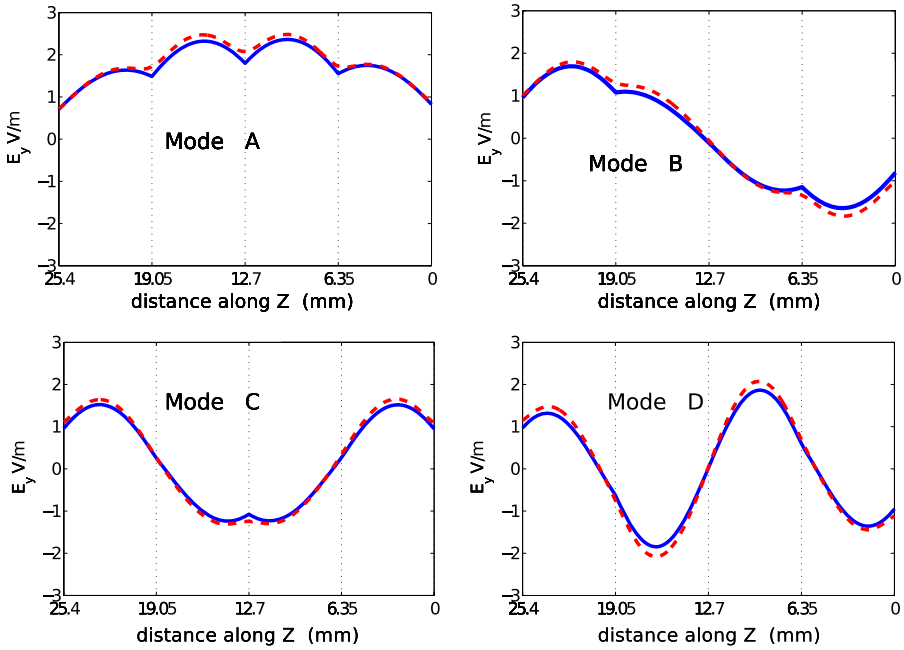

Fig. 4. Field distributions for the four resonance modes of the four open and coupled Fabry-Pérot cavities that can be associated to each of the dielectric slabs in the stacked structure in Fig. 1. The numerical (HFSS, red curves) and analytical (circuit model, blue curves) results show a very good agreement.

the parameters these two limits depend on. Quantitative details about the range of values where the transmission peaks should be expected will be given in the following section.

5. Stacked grids with a large number of layers

In the previous section, a five-grid structure supported by four dielectric slabs has been shown to exhibit four FP-like resonances corresponding to the four coupled FP resonators formed by the reactively-loaded dielectric slabs. We have demonstrated that the circuit model gives a very good quantitative account of the first transmission band, while results are qualitatively correct but quantitatively poor when the frequency increases (second and further bands). We have also mentioned that the highest-frequency peak should not be far from the resonance frequency corresponding to a single slab being half-wavelength thick, in agreement with the theory reported in [8]. This is the practical consequence of the observation of field patterns for the last resonant mode within the first band. However, this is an *a posteriori* conclusion. Moreover, no clear theory has been provided for the position of the first resonance (or, equivalently, for the bandwidth of the first transmission band), which seems to be closely related to the geometry of the grids. The application of our model to structures having a large number of slabs (cells along the *z*-direction) can shed some light on the problem. Thus, for instance, we have verified that the behavior of the field distributions for any number of slabs follows patterns similar to those obtained for the four-slab structure. In particular, the field pattern for the first and last resonance peaks has the same qualitative behavior shown for modes A and D of the four-slab structure. We can say that the phase shift from cell to cell along the *z*-direction is close to zero for the first mode and close to π for the last mode (with intermediate values for all the other peaks). As an

#125055 - $15.00 USD Received 4 Mar 2010; revised 26 May 2010; accepted 4 Jun 2010; published 7 Jun 2010

example, the field patterns for the first and last resonance modes within the first transmission band of a nine-slab structure (with 10 grids) is provided in Fig. 5. It is remarkable the similarity of these plots with the field distributions reported in [4, Fig. 4] for a stacked metal/dielectric system operating at optical wavelengths.

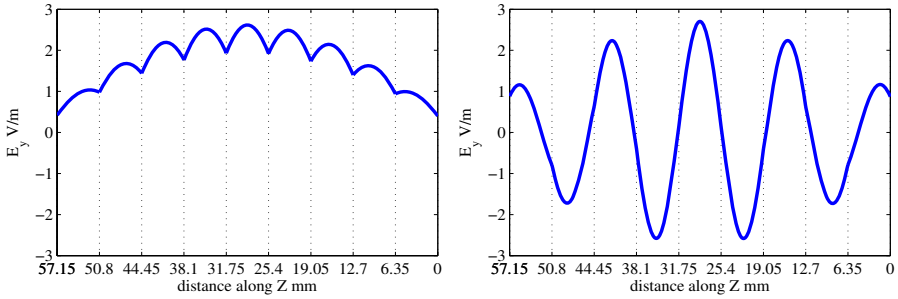

Fig. 5. Field distributions for the first and last resonance peaks (within the first transmission band, which has nine peaks) of a 9 slabs (10 grids) structure. Dimensions of the grids and individual slabs are the same as in Fig. 4. Dielectrics and metals are the same as well.

As the number of identical layers is increased, the number of transmission peaks also increases (there are as many peaks as slabs) but all the peaks lie within a characteristic frequency band whose limits are given by the electrical parameters and dimensions of the unit cell. For instance, the values of the first and last resonance frequencies are tabulated in Table 1 as a function of the number of slabs. The slabs and grids are the same used in the previous figures. Inspection of Table 1 tells us that f_{LB} and f_{UB} tend to some limit values when the number of

Table 1. Frequencies of lower (f_{LB}) and upper (f_{UB}) band edges with respect to the number of layers.

No. of layers	f_{LB} (GHz)	f_{UB} (GHz)
4	7.004	11.610
5	6.780	12.200
6	6.664	12.560
10	6.468	13.190
18	6.380	13.490
36	6.380	13.600

stacked layers increases. Moreover, the resonance frequency of a single slab without considering any grid load is 13.62 GHz for the materials and thicknesses used to compute the values in Table 1. It suggests that the upper limit could be given by that frequency. However, the meaning of the limit value of f_{LB} (6.380 GHz) is not clear. In the following we propose an easy explanation for both the lower and upper limits.

The structure with a large number of cells has a large number of resonances within a finite band. In the limit case of an infinite number of cells, instead of resonances we should have a continuous transmission band, out of which propagation is not possible (forbidden regions). This is expected from the solution of the wave equation in any periodic system. This kind of periodic structures represented by means of circuit elements are commonly analyzed in textbooks of microwave engineering (see, for instance, [22]). The unit cell of the infinite periodic

#125055 - $15.00 USD Received 4 Mar 2010; revised 26 May 2010; accepted 4 Jun 2010; published 7 Jun 2010

structure resulting of making infinite the number of slabs of our problem is shown in Fig. 2(c). If, for simplicity, losses are ignored in the forthcoming discussion and the propagation factor for the Bloch wave is written as $\gamma = \alpha + j\beta$, the following dispersion equation of the periodic structure is obtained following the method reported in [20, 22]:

$$\cosh(\gamma t_d) = \cos(k_d t_d) + j\frac{Z_d}{2Z_g}\sin(k_d t_d) \tag{4}$$

where $k_d = \omega\sqrt{\varepsilon_r}/c$. For those frequencies making the RHS of (4) greater than -1 and smaller than +1, the solution for γ is purely imaginary ($\gamma = j\beta$) as it corresponds to propagating waves in a transmission band. For other frequency values the solution for γ is real, thus giving place to evanescent waves (forbidden propagation or band gaps). For a given transmission band the upper limit is given by the condition

$$\cosh(\gamma t_d) = -1 \tag{5}$$

which is fulfilled by $\beta t_d = \pi \quad (\alpha = 0)$, namely, a phase shift of π radians in the unit cell. The frequency at which this condition appears is given by $\cos(k_d t_d) = -1$, $\sin(k_d t_d) = 0$, which corresponds to the frequency of resonance of a single slab without grid, $k_d t_d = \pi$. This condition is fully consistent with our previous observation in the finite structure of an upper-band limit governed mostly by the thickness of the dielectric slab with no influence of the grid and with a phase shift of the field of π between adjacent layers. On the other hand, the lower limit is given by the condition

$$\cosh(\gamma t_d) \equiv \cos(k_d t_d) + j\frac{Z_d}{2Z_g}\sin(k_d t_d) = 1\,. \tag{6}$$

The condition $\cosh(\gamma t_d) = 1$ is trivially satisfied by $\gamma t_d = 0, \quad (\beta = \alpha = 0)$; namely, a null phase shift in the unit cell, which is in agreement with our previous observation for the field pattern of the lowest-frequency peak. The frequency where the above condition appears clearly depends on the specific value of the grid impedance, Z_g.

Solving the dispersion Eq. (4) we can obtain the Brillouin diagram for any desired band. This has been done in Fig. 6 for the first transmission band of the structure under study, which occurs at low frequencies within the limits of homogenization of the proposed circuit model. Numerical results obtained via commercial software CST [23] have been superimposed to verify the validity of the analytical data. It is clear that the lower limit of the calculated transmission band coincides with the first resonance frequency of the finite structures when the number of cells is large enough. Thus, the range of frequencies where the peaks are expected for a finite stacked structure can be analytically and accurately estimated from Bloch analysis [22] using the proposed circuit model. In particular, the influence of the grid impedance on the lower limit of the transmission band can be obtained from this analysis. The same model explains why the upper limit is solely controlled by the thickness of the slabs. Thus, our analysis gives satisfactory qualitative and quantitative answers to our initial question of what controls the limits of the transmission band. It is worth mentioning here that the second band (or any higher-order band) is not just the second harmonic of the first one: a Bloch wave analysis must be carried out to obtain the actual limits. However, for higher-order transmission bands, the inductive grid could be a poor model that should be corrected by a more accurate value of the loading grid impedance. However, this simple analysis cannot be extended beyond the frequency range where multimode operation arises in the parallel-plate waveguides connecting the grids. In such case the simple transmission line with characteristic impedance Z_d would not be enough to account for the complex higher-order modal interactions between adjacent grids. Fortunately, the frequency region where the model proposed in this paper works properly turns out to be the most interesting region for practical purposes, provided that non-diffracting operation is required (*i.e.*, if higher-order grating lobes are precluded).

#125055 - $15.00 USD Received 4 Mar 2010; revised 26 May 2010; accepted 4 Jun 2010; published 7 Jun 2010

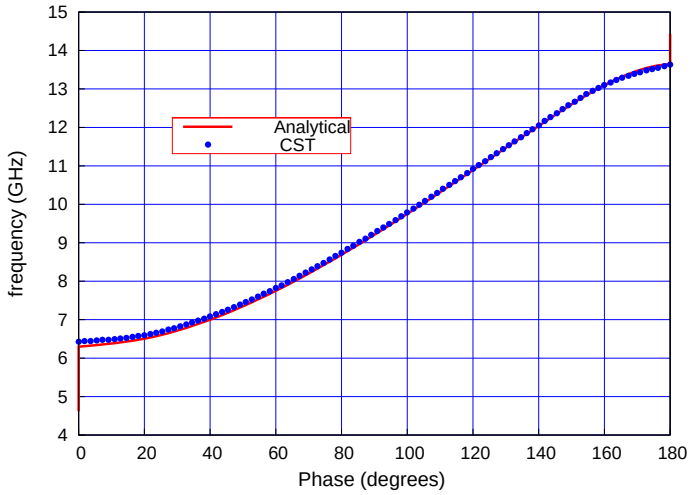

Fig. 6. Brillouin diagram for the first transmission band of an infinite periodic structure (1-D photonic crystal) with the same unit cell as that used in the finite structure considered in Table 1. Numerical results were generated using the commercial software CST [23].

6. Conclusion

This work has shown that the study of the wave propagation along stacked metallic grids separated by dielectric slabs can be carried out analytically with negligible computational effort making use of a simple circuit model. The circuit model remains valid even at frequencies for which the closed-form expressions that account for the influence of the grids are not valid; although in such a case better estimations of grid impedances are required. The main characteristics of the transmission bands (frequencies of the lower and upper resonances) are directly related to the behavior of the infinite 1-D periodic photonic crystal resulting from the use of an infinite number of unit cells. In this case the transmission bands and the band-gaps are accurately determined by means of circuit concepts and textbook analysis methods. The model is valid in the non-diffracting frequency region, far apart from the onset of the first grating lobe.

Acknowledgments

This work has been supported by the Spanish Ministerio de Ciencia e Innovación and European Union FEDER funds (projects TEC2007-65376 and Consolider Ingenio 2010 CSD2008-00066), and by the Spanish Junta de Andalucía (project TIC-4595). Francisco Medina would like to acknowledge the financial support from Spanish Ministerio de Ciencia e Innovación (mobility grant PR09-0405) during his stay at Queen Mary University of London, under supervision of Prof. Yang Hao. Alastair Hibbins and Celia Butler would like to acknowledge the financial support of the EPSRC (UK) and QinetiQ for supporting this work through APH's Advanced Research Fellowship and CAMB's Industrial CASE studentship.